RESEARCH ARTICLE

Removal of chlorpheniramine and variations of nitrosamine formation potentials in municipal wastewaters by adsorption onto the GO-Fe$_3$O$_4$

Chih-Hsien Lin[1] · Chi-Min Li[1] · Chun-Hu Chen[2] · Wei-Hsiang Chen[1] 🆔

Abstract

Chlorpheniramine is a pharmaceutical pollutant and a precursor of carcinogenic nitrosamines during disinfection/oxidation. In our previous study, graphene oxide coated with magnetite (GO-Fe$_3$O$_4$) was capable of removing chlorpheniramine in deionized water by adsorption. This study investigated the removal of chlorpheniramine and its nitrosamine formation potentials (FPs) by adsorption onto magnetic GO-Fe$_3$O$_4$, with respect to the influence by using real municipal wastewaters as the background. In the results, the adsorption performances of chlorpheniramine in wastewaters decreased in the order: GO-Fe$_3$O$_4$ suspension > GO-Fe$_3$O$_4$ particles > activated carbon. Chlorpheniramine adsorptions on GO-Fe$_3$O$_4$ particles and activated carbon were reduced by using real wastewaters as the background, whereas chlorpheniramine adsorption on GO-Fe$_3$O$_4$ suspension was enhanced due to the effects of surface charge on GO-Fe$_3$O$_4$ and ionic strength variation in water. The fittings of adsorption isotherms indicated that the wastewater background reduced the surface heterogeneity of GO-Fe$_3$O$_4$ suspension and improved the adsorption performance. Appreciable removal efficiencies of NDMA and other nitrosamine FPs were observed when GO-Fe$_3$O$_4$ particles were added in real wastewaters. However, when chlorpheniramine was present in wastewaters, chlorpheniramine adsorption and degradation reaction simultaneously occurred on the surface of GO-Fe$_3$O$_4$, increasing NDMA and other nitrosamine FPs in wastewaters after GO-Fe$_3$O$_4$ addition for chlorpheniramine adsorption. The assumption was further demonstrated by observing the NDMA-FP increase during chlorpheniramine adsorption on GO-Fe$_3$O$_4$ in deionized water. GO-Fe$_3$O$_4$ is a potential adsorbent for chlorpheniramine removal. Nevertheless, the low treatment efficiencies at high doses limit its application for nitrosamine FP adsorptions in real wastewaters.

Keywords Graphene oxide · Magnetite · Chlorpheniramine · Nitrosamine · Formation potential · Adsorption

Introduction

Graphene is a flourishing material with two-dimensional crystalline allotrope of carbon in many scientific areas, displaying

exceptional electrical, mechanical, semi-metal, and optical properties (Geim and Novoselov 2007; Stankovich et al. 2006; Zhao et al. 2014). Graphene oxide (GO) is a derivative of graphene prepared by a chemical modification that adds a number of oxygen-containing groups on the basal planes and sheet edges (Lee et al. 2013; Wu et al. 2015). Given its stability in water, high specific surface areas, and modifiable functional groups (Fan et al. 2013; Yang et al. 2013), the interest grows in potential applications of GO in water purification. Using pristine GO faces the challenge that this nano-sized material is difficult to separate from water. One solution is to modify GO with different metal oxides such as MnO$_2$ (Chen et al. 2010; Fan et al. 2011) or ZnO (Chung et al. 2010; Zhang et al. 2009), so magnetic composites are removable from the water after treatment through a magnetic field. GO-Fe$_3$O$_4$ composites draw attention due to its excellent magnetic

---

✉ Wei-Hsiang Chen
   whchen@mail.nsysu.eu.tw

[1] Institute of Environmental Engineering, National Sun Yat-sen University, Kaohsiung 804, Taiwan

[2] Department of Chemistry, National Sun Yat-sen University, Kaohsiung 804, Taiwan

properties, stability in water at neutral pH values, and adsorption performances toward organic and inorganic compounds (Fan et al. 2013; Li et al. 2017; Wu et al. 2015).

Chlorpheniramine (CAS 132-22-9) is one commonly used antihistamine to treat an upper respiratory infection and allergic conditions in human health and small-animal veterinary practices (Li et al. 2011). With a high solubility, rapid dissolution rate, and efficient permeability, chlorpheniramine occurs in aquatic environments and poses adverse effects on ecological systems and public health (Moreno et al. 2010; Roberts et al. 2016; Xia et al. 2014). Chlorpheniramine identification in wastewater treatment plants has been widely reported (Lv et al. 2015; Roberts et al. 2016). Chlorpheniramine is also considered as one priority pharmaceuticals for future study of human and environmental health (Boxall 2004). In addition, chlorpheniramine is known to form N-nitrosodimethylamine (NDMA) during disinfection/oxidation in water treatments (Lv et al. 2015). The molar conversion ratio of NDMA from chlorpheniramine was approximately 5.2–5.5% during chloramine disinfection (Shen and Andrews 2011a).

With increasing concern for nitrogenous disinfection byproducts (NDBPs), nitrosamines are a group of polar and semi-volatile organic compounds frequently detected in drinking waters and wastewaters worldwide (Chen et al. 2018; Shah et al. 2012; Wang et al. 2016). One important source of the emerging contaminants is municipal wastewater effluents (Mitch et al. 2005; Shah et al. 2012). During chlorination (Chen et al. 2015), chloramination (Liu et al. 2014), ozone (Yang et al. 2009), or catalytic reactions on the surface of activated carbon (Padhye et al. 2011), nitrosamines are formed from a large number of potential precursors in municipal wastewater effluents. Nitrosamines are notorious for their potent carcinogenicity. For example, NDMA and nitrosodimethylamine are classified as a B2 (probable human) carcinogen by the U.S. Environmental Protection Agency (USEPA) (USEPA 2017). The International Agency for Research on Cancer (IARC) listed NDMA and NDEA in group 2A which are possibly carcinogenic to humans (IARC 1987).

Studies have reported that via $\pi - \pi$ bonding and cation−π bonding, pharmaceutical pollutants such as tetracycline (Lin et al. 2013) and sulfonamide (Luo et al. 2011) are efficiently adsorbed onto the surface of GO-Fe$_3$O$_4$ and removed from the aqueous phase. However, the myriad wastewater constituents may adversely affect the adsorption, as certain compounds exhibit nitrosamine FPs that represent other target pollutants for removal. Our previous study observed the efficient adsorption of chlorpheniramine onto magnetic GO-Fe$_3$O$_4$ in deionized water (Li et al. 2017). This study further investigated the adsorption of chlorpheniramine and its nitrosamine FPs with respect to the influence by using real wastewaters (e.g., municipal or medical wastewater) as the background. GO-Fe$_3$O$_4$

composite suspension and particles were synthesized by co-precipitation. The variation of chlorpheniramine and nitrosamine FP concentrations in deionized water and real wastewaters before and after addition of GO-Fe$_3$O$_4$ was analyzed for comparison by batch experiments.

Materials and methods

Materials

Graphite powder (99.95%) and powdered activated carbon (PAC) were supplied by Acros Organics and Alfa Aesar, respectively. Fisher Scientific provided chemicals needed for preparation of GO-Fe$_3$O$_4$, including ferrous chloride (FeCl$_2$), ferric chloride (FeCl$_3$), ammonium chloride (NH$_4$Cl), sodium nitrate (NaNO$_3$), potassium permanganate (KMnO$_4$), hydrogen peroxide (H$_2$O$_2$), and hydrogen chlorite (HCl). Chlorpheniramine (25 g, 99%) and bromopheniramine (100 mg, 99%) standards were obtained from Alfa Aesar. Nitrosamine standards were obtained from Chem Service. Deuterated NDMA (NDMA-d$_6$) and deuterated nitrosodipropylamine (NDPA-d$_{14}$) were purchased from Chem Service. NDMA-d$_6$ was added prior to solid phase extraction (SPE) to monitor the method performance. NDPA-d$_{14}$ was used as an internal standard for quantification of native compounds in instrumental analyses. Solid-phase extraction cartridges were purchased from Sigma-Aldrich. The cartridges are suggested in Method 521 published by the USEPA for nitrosamine analysis (USEPA 2004). Sodium hydroxide (NaOH) and sulfuric acid (H$_2$SO$_4$) (Fisher Scientific) were used for pH adjustment. All reagents applied in this study were analytical grade and used without purification.

GO-Fe$_3$O$_4$ preparation

Following the method in our previous study (Li et al. 2017), the Hummers method was modified to prepare GO suspension from bulk flake graphite crystals. The GO suspension was used to synthesize GO-Fe$_3$O$_4$ composites. Our previous study compared the chlorpheniramine adsorption on GO-Fe$_3$O$_4$ prepared with different mass ratios of Fe$_3$Cl to GO in deionized water. Given the experiences, the GO-Fe$_3$O$_4$ was prepared with a FeCl$_3$ to GO ratio of 2.5 in this study. GO suspension (40 mg, dry weight) was mixed with a FeCl$_3$ and FeCl$_2$ solution (50 ml, the mass ratio of FeCl$_3$ to FeCl$_2$ was 2.7). The subsequent steps to collect GO-Fe$_3$O$_4$ particles were identical to those described in our previous study. The particles were ground and sieved to a 40-mesh size for being used in the following experiments. Fig. S1 in the supplementary materials shows the X-ray diffraction (XRD), scanning electron microscope (SEM), and Brunauer-Emmett-Teller BET results of GO, GO, and GO-Fe$_3$O$_4$ composites.

Wastewater sampling

Two wastewater treatment plants (WWTP1 and WWTP2) were selected in this study to collect the effluents for the experiments. The total daily flow capacities of WWTP1 and WWTP2 are 12,000 and 14,000 cubic meters per day (CMD), respectively. The municipal wastewater is the main source of WWTP1. The influent of WWTP2 contains industrial and medical wastewaters (40%), municipal wastewater (42%), and stormwater (18%). After equalization as the initial process, the main treatment steps of WWTP1 comprise an up-flow anaerobic fluidized bed reactor, biological contact oxidation reactor, and post-disinfection before the discharge. In WWTP2, the treatment processes consist of activated sludge and sedimentation. The water quality parameters including the conductivity, pH, dissolved oxygen (DO), ammonium, nitrite, nitrate, free and total chlorine, dissolved organic carbon (DOC) concentrations, ultraviolet absorbance at 254-nm wavelength (UV254), and specific ultraviolet absorption (SUVA) of two WWTPs were analyzed, as shown in Table 1.

In WWTP1, with the relatively higher conductivity, DOC, UV254, and SUVA values (Table 1), the wastewater samples were used to study the influence of real municipal wastewater on chlorpheniramine adsorption onto GO-Fe$_3$O$_4$. In WWTP2, the water source is more complex. Nitrosamines are known to be formed from a variety of natural (e.g., natural organic matter) and synthetic precursors (e.g., amine-containing compounds such as herbicides or pharmaceuticals) (Bond et al. 2012; Krasner et al. 2013). The wastewater in WWTP2 is suitable for investigation of the influence of real wastewater on nitrosamine FP removal by GO-Fe$_3$O$_4$. The wastewater in WWTP2 was sampled twice at different times to reduce the

influence of water quality variation on the consistency of our observations given the complexity of its water sources. In two WWTPs, at least 1 L of the effluent was collected. H$_2$SO$_4$ was added in the sample to control the pH below 2, followed by being stored at 4 °C and analyzed in 48 h.

Chlorpheniramine adsorption

Adsorption of chlorpheniramine onto GO-Fe$_3$O$_4$ was investigated in batch experiments by using 50-mL polyethylene centrifuge tubes. Thirty milligrams of GO-Fe$_3$O$_4$ particles, GO-Fe$_3$O$_4$ suspension, or activated carbon was added as the adsorbent. The chlorpheniramine concentration (described in the following discussion) was adjusted to achieve the desired experimental conditions. The experiments were conducted at the optimal pH of 6 by adding NaOH or H$_2$SO$_4$. The experimental conditions were consistent with those in our previous study for comparison of the results in different waters (Li et al. 2017). The solution was continuously and gently shaken for 24 h, followed by centrifugation (4000 rpm, 15 min). At equilibrium, magnetic force was applied to remove GO-Fe$_3$O$_4$ from the aqueous phase. After spiking with bromopheniramine (1 g/L, 10 μL), the solution (20 mL) was pretreated by liquid-liquid extraction. The solvent consisted of dichloromethane and diethyl ether (the volume ratio was 4). The extract was concentrated to 1 mL by rotary evaporator and nitrogen blow down.

Gas chromatography (Agilent 7890B, USA) coupled with mass spectrometry (Agilent 5977A, USA) (GC/MS) was employed for chlorpheniramine analysis. The extract (1 μL) was injected in splitless mode. The temperature of the inlet was 290 °C. Helium was the carrier gas. The flow rate was 1.2 mL/min. The analytes were separated by using a capillary column (HP-5MS, 30 m × 0.25 mm with 0.25-μm film thickness). The oven temperature was programmed as follows: initial temperature of 40 °C, raised to 200 °C at 30 °C/min, then controlled at 300 °C at 15 °C/min. The MS was operated in the electron impact mode. The temperature of the source was 230 °C. The method detection limit (MDL) of chlorpheniramine was approximately 1 μg/L. The accuracy of chlorpheniramine analysis in real wastewaters from WWTP1 was estimated (Fig. S2 in the supplementary materials). The recovery ranged from 92 to 119% ($n = 7$).

Nitrosamine FP adsorption

Adsorption of eight nitrosamine FPs onto GO-Fe$_3$O$_4$ was investigated in batch experiments. Eight nitrosamines of concern included NDMA, N-nitrosomethylethylamine (NMEA), NDEA, NDPA, N-nitrosodibutylamine (NDBA), N-nitrosopyrrolidine (NPYR), N-nitrosopiperidine (NPIP), and N-nitrosomorpholine (NMOR). Chlorpheniramine was injected as the precursor for nitrosamine formation. By

Table 1 Water quality information of the wastewater samples collected in this study

	WWTP1	WWTP2[1]	WWTP2[1]
pH	8.0	7.9	7.9
Conductivity (μs/cm)	1068	645	929
DO (mg/L)	7.4	7.1	5.7
DOC (mg/L)	8.3 ± 0.1	6.9 ± 0.1	7.1 ± 0.1
UV$_{254}$ (cm^{-1})	0.26 ± 0.02	0.10	0.10
SUVA (L/mg-m)	3.15 ± 0.24	1.47 ± 0.01	1.37 ± 0.03
NO$_3$-N (mg/L)	< 0.10	3.95 ± 0.15	0.55 ± 0.05
NO$_2$-N (mg/L)	0.06 ± 0.01	0.04 ± 0.01	0.16 ± 0.01
NH$_4$-N (mg/L)	50.0 ± 3.0	11.4 ± 0.7	16.3 ± 0.5
Free chlorine (mg/L as Cl)	0.13 ± 0.01	N.A.	N.A.
Total chlorine (mg/L as Cl)	0.14 ± 0.00	N.A.	N.A.

N.A. not available

[1] WWTP2 was sampled twice at two different times in this study to understand the water quality variation given the complexity of its water sources

running the experiments in a sealed 1.2-L amber jar at pH 7 for 24 h under dark condition, the solution was filtered by using a glass fiber filter. Monochloramine (2 mM) was added for complete oxidation of chlorpheniramine and other precursor compounds present in wastewaters for nitrosamine formation (Chen et al. 2014; Kadmi et al. 2015). Monochloramine was prepared before experiments by adding sodium hypochlorite in an ammonium chloride solution. The molar ratio of chlorine to nitrogen was 1:1.2 to limit excess hypochlorite causing breakpoint chlorination. The pH was 8.5 to minimize the degradation of monochloramine. The reaction time was 7 days. Sodium dihydrogen phosphate was added as a buffer. Before solid phase extraction, NDMA-d$_6$ (10 mg/L, 24 μL) was spiked. A *cartridge* packed with coconut charcoal (2 g) in a polypropylene tube (6 mL) was used for solid phase extraction of nitrosamines from the supernatant. Dichloromethane (15 mL) was applied to extract nitrosamines from the cartridge. The extract was concentrated to 0.5 mL by nitrogen blowdown.

GC/MS (Agilent 7890B, USA; Agilent 5977A, USA) was employed for nitrosamine FP analysis. The extract (2 μL) was injected in splitless mode at 280 °C. The GC was equipped with a capillary column (HP-5MS, 30 m × 0.25 mm with 0.25-μm film thickness). The oven temperature was programmed as follows: 40 °C held for 1 min, ramped to 100 °C at 10 °C/min, ramped to 180 °C at 15 °C/min, then 260 °C at 35 °C/min. The temperature of the source was 230 °C. Besides the use of surrogate (NDMA-d$_6$) and internal standard (NDPA-d$_{14}$), the method of standard addition was applied to reduce the matrix effect by background noises of interfering peaks, unequivocally identifying nitrosamines in complex wastewater matrices. The MDLs of eight nitrosamines ranged from 1.4 to 3.7 ng/L.

Adsorption isotherm

Adsorption isotherm is a mathematical approach to describe the experimentally determined sorption data of a compound between aqueous and solid phases under the isothermal state. In the experiments, 30 mg of adsorbent (GO-Fe$_3$O$_4$ or activated carbon) was added in the chlorpheniramine solution (from 10 to 200 mg/L) at pH 6. The solution was then continuously and gently shaken for 24 h, followed by an analysis of the residual chlorpheniramine concentration. Two widely used adsorption models, namely the Langmuir (Eq. 1) and Freundlich isotherms (Eq. 2), were used to describe the adsorption of chlorpheniramine and nitrosamine FPs onto GO-Fe$_3$O$_4$. The Langmuir adsorption model explains adsorption of a single solute onto a series of equivalent sites on a homogeneous solid surface. Each site holds a single solute. No interaction occurs between the solute and the site. The Freundlich adsorption model is applied for non-ideal

sorption on heterogeneous surfaces and multilayer sorption (Schwarzenbach et al. 2003).

$$q = \frac{q_m K_L C}{1 + K_L C} \tag{1}$$

$$q = K_F C^n \tag{2}$$

where q and C represent the concentrations of chlorpheniramine or nitrosamine FPs on GO [mg/g] and in aqueous phase [mg/L], respectively; q_m represents the total number of surface sites per mass of sorbent [mg/g]; K_L is the Langmuir constant [L/kg], which is defined as the equilibrium constant of sorption reaction and implies a constant sorbate affinity for all surface sites. K_F and n represent the Freundlich capacity factor [(mg/kg)/(mg/L)^n] and model exponent (Freundlich constant), respectively.

Results and discussion

Adsorption isotherm

Our previous study has demonstrated the efficient adsorption of chlorpheniramine onto the GO-Fe$_3$O$_4$ suspension or particles in deionized water (Li et al. 2017). The adsorption performance was enhanced when the particles were prepared with a low Fe$_3$O$_4$ to GO mass ratio to increase the specific surface area and nano-pore volumes. To investigate its practicability in real wastewaters, the adsorption of chlorpheniramine on GO-Fe$_3$O$_4$ particles or suspension in real wastewaters was investigated, as shown in Fig. 1. High chlorpheniramine concentrations (from 10 to 120 mg/L) were employed to observe the adsorption isotherms. The adsorbed concentration (q_e) was determined by estimating the mass of chlorpheniramine adsorbed on the surface of GO. An experiment using activated carbon prepared at the same mesh size was conducted simultaneously (triangles in Fig. 1).

The maximum adsorption concentrations decreased in the order: GO-Fe$_3$O$_4$ suspension > GO-Fe$_3$O$_4$ particles > activated carbon. These observations were fitted in Freundlich and Langmuir adsorption models (Fig. 1 and Table 2). Both adsorption models fitted the observation well, as the Freundlich isotherm exhibited slightly better results. The limited differences between the two adsorption models suggested that although GO-Fe$_3$O$_4$ is a composite containing two different materials, the surface could be relatively homogeneous for the adsorption of chlorpheniramine.

Table 2 lists the parameters by fitting the observed data in the Freundlich and Langmuir isomerism models. In the result, Freundlich and Langmuir models both fitted the observed data well, as the results by the Freundlich model were slightly better. The values of q_m (the total number of the surface site per mass of sorbent) (except the wastewater experiment using GO-Fe$_3$O$_4$

Fig. 1 Chlorpheniramine adsorption on GO-Fe$_3$O$_4$ suspension, GO-Fe$_3$O$_4$ particles, or activated carbon in wastewaters. The black and red lines depict the fittings for the Freundlich and Langmuir models, respectively. The solid, long-dashed, and short-dashed lines represent the results for GO-Fe$_3$O$_4$ suspension, GO-Fe$_3$O$_4$ particle, and activated carbon, respectively
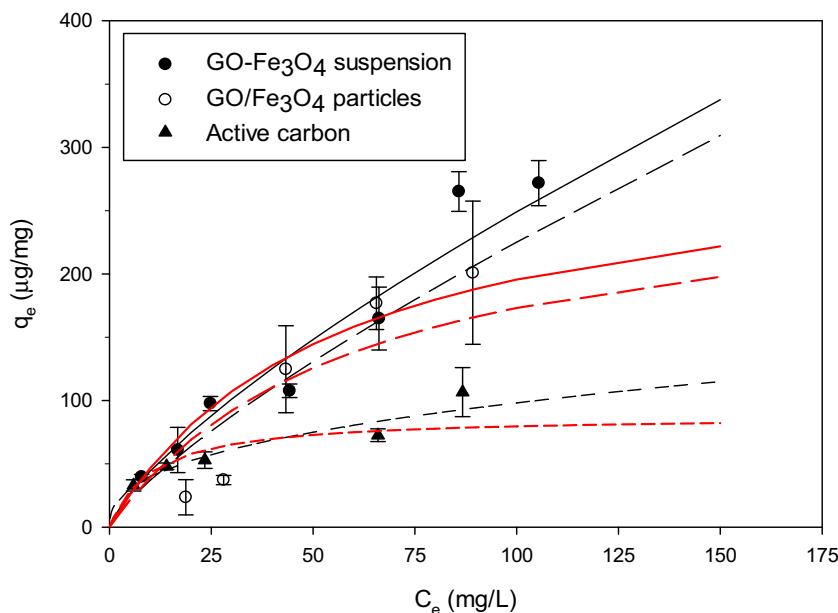
suspension), K_L (the Langmuir constant), and K_F (the capacity factor in the Freundlich model) decreased in the wastewater experiments, as expected. The parameter n in the experiments using real wastewaters, which is an index of the diversity of free energies associated with the sorption of the solute (i.e., chlorpheniramine) by multiple components of a heterogeneous sorbent (i.e., GO-Fe$_3$O$_4$) (Carter et al. 1995; Schwarzenbach et al. 2003), was significantly greater than those in the deionized water experiments. The n values were increased 1.69 and 2 times for the GO-Fe$_3$O$_4$ particles and suspension, respectively, whereas the increase was only 1.29 times for activated carbon. The larger Freundlich constants in real wastewater experiments inferred that the compounds in real wastewaters such as organic substances potentially enhanced the free energies of further chlorpheniramine sorption onto the surface of GO-Fe$_3$O$_4$.

Influence of real wastewaters

Figure 2 compares the chlorpheniramine adsorption onto the GO-Fe$_3$O$_4$ particles, suspension, and activated carbon between real wastewater and deionized water. The initial chlorpheniramine concentrations ranged from 10 to 200 mg/L. In the results, the GO-Fe$_3$O$_4$ particles and suspension exhibited better adsorption performances than the activated carbon. The presence of real wastewater reduced the chlorpheniramine adsorption on three adsorbents, notably on the GO-Fe$_3$O$_4$ particles and activated carbon. It was reported that the chlorpheniramine removal by adsorption on activated carbon decreased from 75 to 40% (q_e was reduced from 190 to 101 mg/g) when the background was changed from deionized water to 90% surface water plus 10% wastewater effluent (Hanigan et al.

Table 2 Adsorption isotherm models used to fit the observed sorption data

		Langmuir			Freundlich		
		q_m (μg/mg)	K_L (L/mg)	R^2	n	K_F ((μg/mg)/(mg/L)^n)	R^2
Wastewater[a]	Particles	277.8	0.02	0.96	0.78	6.09	0.97
	Suspension	303.0	0.02	0.96	0.75	7.89	0.96
	Activated carbon	87.7	0.01	0.92	0.39	16.42	0.94
Deionized water[a, b]	Particles	303.0	0.08	0.98	0.29	72.8	0.98
	Suspension	154.0	0.17	0.98	0.25	54.00	0.98
	Activated carbon	120.5	0.35	0.92	0.17	58.93	0.98

[a] The experimental pH was 6. The contact time was 24 h. The adsorbents were controlled at 40-mesh size

[b] Data source: (Li et al. 2017)
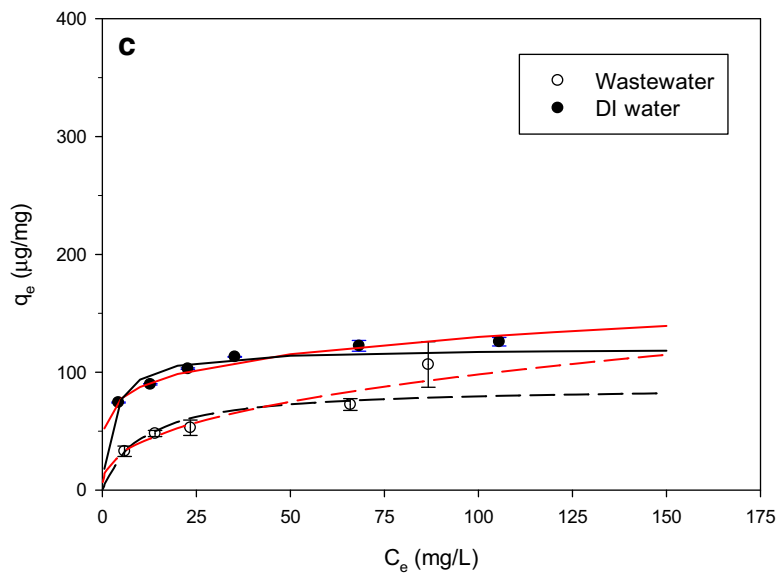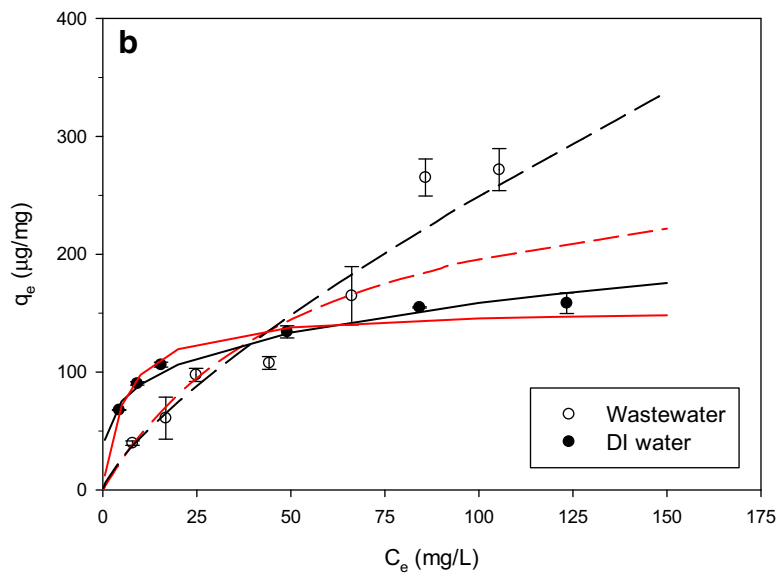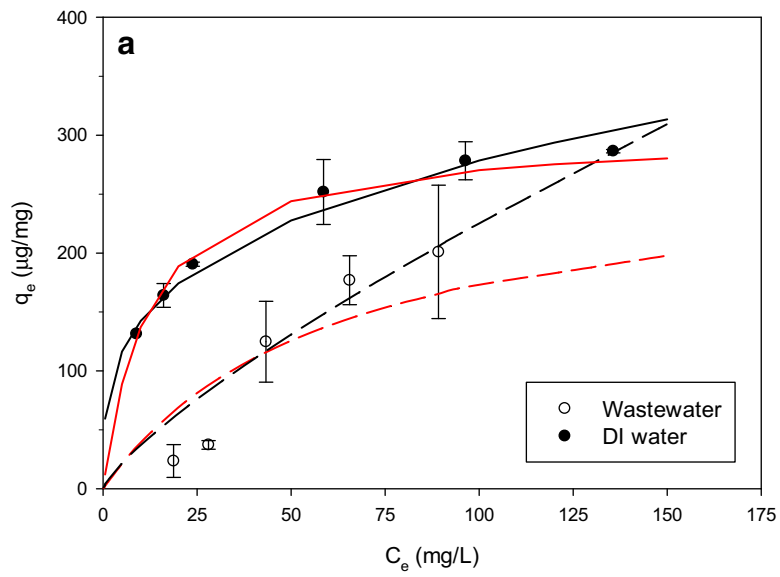
◀ **Fig. 2** Chlorpheniramine adsorption on (**a**) GO-Fe$_3$O$_4$ suspension; (**b**) GO-Fe$_3$O$_4$ particles; and (**c**) activated carbon in wastewaters (this study) and deionized water (Li et al. 2017). The black and red lines depict the fittings for the Freundlich and Langmuir models, respectively. The solid, long-dashed, and medium-dashed lines represent the fittings for GO-Fe$_3$O$_4$ suspension, GO-Fe$_3$O$_4$ particle, and activated carbon, respectively

2012). Certain pharmaceuticals that form nitrosamines showed similar results, whereas the inhibition was limited in the experiments using ranitidine (a medication which decreases stomach acid production) and tetracycline (an antibiotic used to treat a number of infections) (Apul et al. 2013). Competition between organic substances in wastewaters and certain functional groups of the pharmaceuticals for adsorption sites on activated carbon or GO-Fe$_3$O$_4$ is one explanation (Hanigan et al. 2012).

In Fig. 2 b, the chlorpheniramine adsorption on GO-Fe$_3$O$_4$ suspension in real wastewater was enhanced and higher than that in deionized water at high chlorpheniramine concentrations. In Table 2, the n value in the Freundlich equation and the q_{max} value in Langmuir equation were both larger in the real wastewater experiment when GO-Fe$_3$O$_4$ suspension was employed. Our previous study indicated that the electrostatic interaction is the main mechanism involved during chlorpheniramine adsorption onto GO-Fe$_3$O$_4$ suspension, as the specific surface area and micropore volume are more critical for chlorpheniramine adsorption on GO-Fe$_3$O$_4$ particles (Li et al. 2017). Humic and fulvic acids are the major compositions (40%–60%) in natural organic matters (Schlautman and Morgan 1993). Due to carboxylic and phenolic groups in the humic and fulvic acids, organic substances have negative charges on their surfaces (Zhou et al. 2014). The zeta potential of GO-Fe$_3$O$_4$ suspension used in this experiment ranged from − 35.1 to − 15.1 mV between pH 4 and 10 (Li et al. 2017). The negative charges on the surfaces of both organic substances and GO-Fe$_3$O$_4$ suspension potentially limited the competition for adsorption sites on GO-Fe$_3$O$_4$ suspension between chlorpheniramine and organic substances. Apul et al. suggested that the oxygen-containing functional groups increased the stability of GO in the aqueous phase, diminishing the negative effect of organic substances on the adsorption behaviors on GO (Apul et al. 2013).

Ionic strength is another explanation for the enhanced chlorpheniramine adsorption in wastewaters at high chlorpheniramine concentrations. The ionic strength was increased from 10^{-3} to 1.8×10^{-2} M when the background was changed from deionized water to wastewater in this experiment. The solubility change of chlorpheniramine by salting out as well as the variation of heterogeneity and electrical double layer thickness on the surface of *GO-Fe$_3$O$_4$* suspension by organic substances (Li et al. 2012) contributed to the enhanced adsorption of chlorpheniramine in real wastewaters.

Removal of nitrosamine FPs in wastewaters

The wastewaters collected in WWTP2 were used to investigate the removal of nitrosamine FPs by adsorption using the GO-Fe$_3$O$_4$ particles. Fig. S3 in the supplementary materials shows the occurrences of four nitrosamine FPs including NDMA-FP (276 and 94 ng/L in two samplings), NPIP-FP (446 and 247 ng/L in two samplings), NMOR-FP (277 and 18 ng/L in two samplings), and NDBA-FP (83 ng/L and non-detected in two samplings) in the wastewaters collected in WWTP2. A strong correlation ($r = 0.88$) was present between the nitrosamine FP distributions between two sampling events. Medical wastewater was one major source of WWTP2 and the treated water was not chlorinated, resulting in the high levels of nitrosamine FPs in the results.

Development of studies regarding the removal of different nitrosamine FPs has started for years. Sacher et al. have shown 50% and 90% NDMA-FP reduction in multiple surface waters exposed to PAC at a dose of 5 and 20 mg/L for 7 days, respectively (Sacher et al. 2008). Hanigan et al. reported that 37% and 69% NDMA-FP reduction in municipal wastewater effluents by both PAC (37%) and granular activated carbon (GAC, 59%) at a 4-h contact time. Reduction of 60–80% NDMA-FP was demonstrated in the pilot- and full-scale studies using GAC (Hanigan et al. 2012).

In this work, Fig. 3 a and b illustrate the variations of four nitrosamine FPs in the wastewaters (500 mL) from WWTP2 in two samplings after the addition of GO-Fe$_3$O$_4$ (30 mg) in the experiments, respectively. In Fig. 3 a, the adsorption capacities of the GO-Fe$_3$O$_4$ for NDMA-FP, NPIP-FP, NMOR-FP, and NDBA-FP were 3.98, 3.12, 4.46, and 1.31 ng/mg, respectively. In Fig. 3 b, the adsorption capacities of the GO-Fe$_3$O$_4$ for NDMA-FP, NPIP-FP, NMOR-FP, and NDBA-FP were 0.59, 3.34, 0.37 ng/mg, and not-detected, respectively. The removal percentages of NDMA-FP, NPIP-FP, NMOR-FP, and NDBA-FP were $29 \pm 12\%$, $26 \pm 6\%$, $46 \pm 1\%$, and 44%, respectively. Nitrosamine FPs with larger molecular weights exhibited greater removal efficiencies by the GO-Fe$_3$O$_4$ ($r = 0.75$). However, it is shown that the dose of 60 mg/L of the GO-Fe$_3$O$_4$ was significantly higher with lower NDMA-FP removal than activated carbon.

Besides activated carbon, Uzun et al. investigated the removals of NDMA-FP by different treatment technologies at 9 drinking water treatment plants (Uzun et al. 2017). The average NDMA-FP removals by aluminum clarification, PAC addition at high doses (> 4 mg/L), simultaneous application of chlorine and chlorine dioxide, reverse osmosis, and microfiltration were 12–30%, 41–55%, 51–61%, 81%, and 7%, respectively. Chen et al. reported that pre-chlorination in drinking water treatment plants removed the NDMA-FP in the source water by 38–57%, whereas the NDMA-FP was limitedly changed (8%) or increased (− 98%) during pre-ozonation (Chen et al. 2016). As to other nitrosamine FPs, Takeuchi et al.

Fig. 3 Nitrosamine FPs detected in the wastewaters collected in two samplings (**a** and **b**) before and after the addition of GO-Fe$_3$O$_4$ particles. The numbers in brackets indicate the adsorption capacities of GO for different nitrosamine FPs
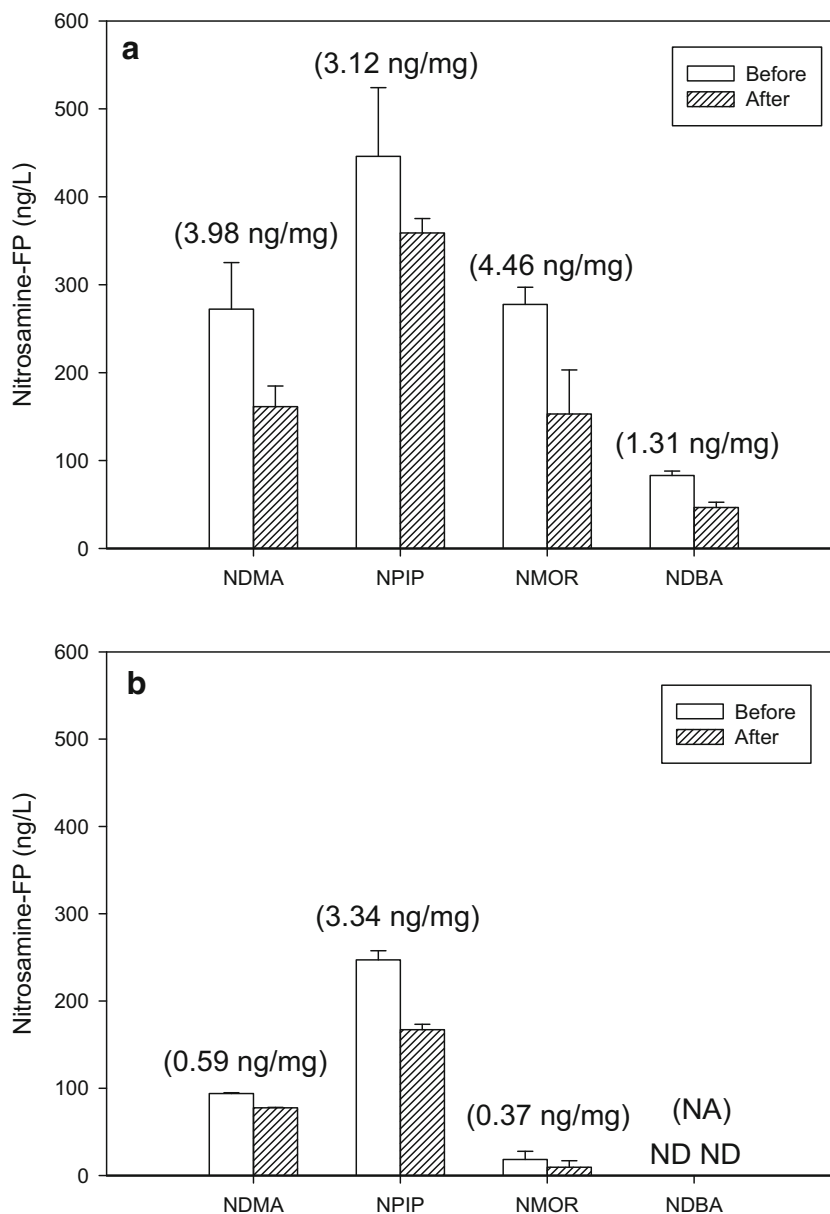
observed that the reduction rates of NPYR-FP were 64% by microfiltration, 1% by nanofiltration, and 36% by RO, and those of NDEA-FP were negligible by MF, 82% by NF, and 7% by RO (Takeuchi et al. 2018). The lower treatment efficiencies at high dose somehow limit the application of GO-Fe$_3$O$_4$ for removal of nitrosamine FP in real wastewaters.

Removal of nitrosamine FPs posed by chlorpheniramine in wastewaters

Chlorpheniramine is a known NDMA precursor. Figure 4 shows the variations of four nitrosamine FPs in the wastewater from WWTP2 spiked with chlorpheniramine and the GO-Fe$_3$O$_4$, respectively. The molar yield of NDMA from chlorpheniramine was reported to be around 2–4% (Liu

et al. 2014; Shen and Andrews 2011a; Shen and Andrews 2011b). In the results, the NDMA-FP was significantly increased from 93 to 272 ng/L (Fig. 3a, b) to 9.9–23.4 μg/L (Fig. 4a, b) by adding chlorpheniramine in the wastewaters. The NDMA-FP increases fell within the reasonable expectation, as 21,610–43,220 ng/L of NDMA-FP could be formed by adding 14.6 μM of chlorpheniramine (a concentration within the range of the adsorption isotherm experiments above) with NDMA molar yield of 2–4%.

After the GO-Fe$_3$O$_4$ addition, the NMOR-FP (Fig. 4a) and NPIP-FP (Fig. 4b) were limitedly changed ($p > 0.05$), while the NPIP-FP (Fig. 4a) and NMOR-FP (Fig. 4b) were significantly reduced and increased (presumably relevant to possible precursors in the wastewater), respectively ($p < 0.01$).

Fig. 4 Nitrosamine FPs detected in the wastewaters collected in two samplings (**a** and **b**) spiked with chlorpheniramine before and after the adsorption by the GO-Fe_3O_4 particles. The numbers in brackets indicate the adsorption capacities of GO for different nitrosamine FPs
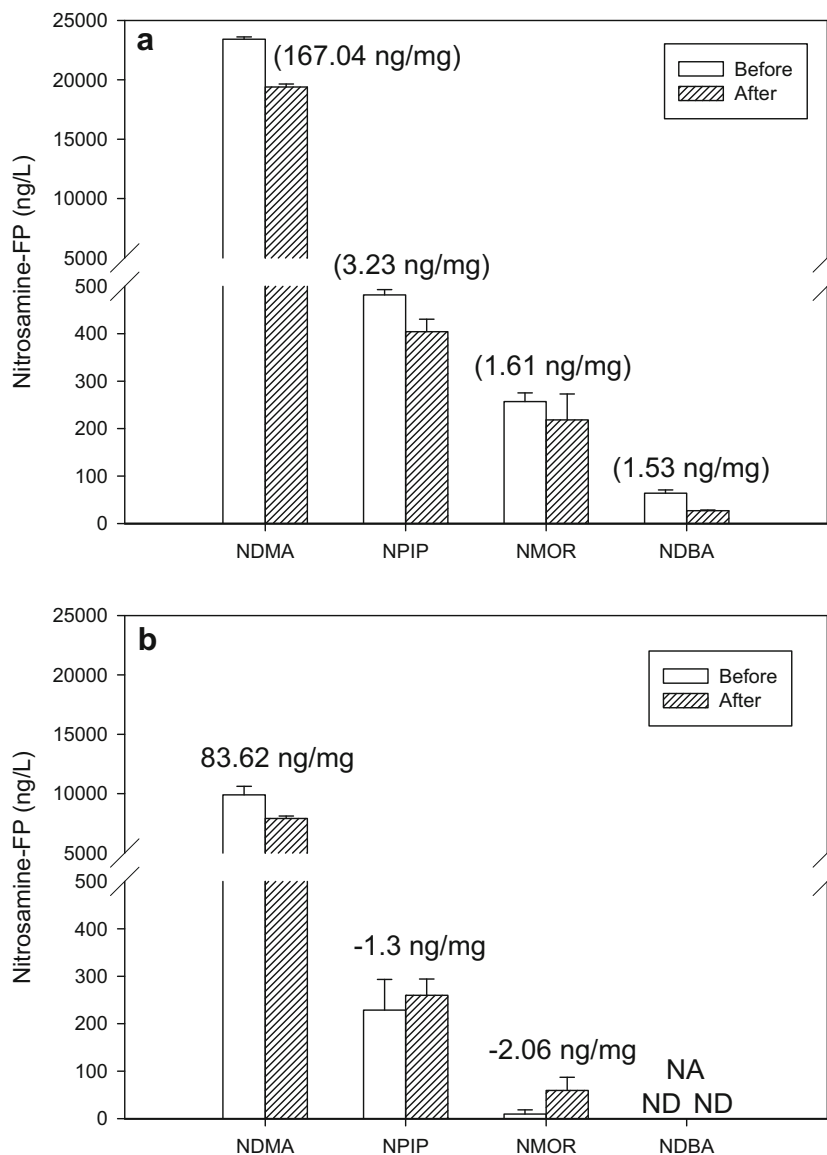
However, after the adsorption onto GO-Fe_3O_4, the NDMA-FP ranging from 7896 to 19,400 ng/L was analyzed. The maximum adsorption capacity of GO-Fe_3O_4 for chlorpheniramine was reported as 317–470 mg/g (Li et al. 2017). With this information, chlorpheniramine added in the wastewaters was supposed to be removed (~20.5 μM), significantly reducing the NDMA-FP after adsorption. In Fig. 4 a and b, the NDMA-FP after adsorption ranged from 7896 to 19,400 ng/L. The adsorption removal of NDMA-FP onto GO-Fe_3O_4 was only 83.6–167.0 ng/mg in the experiments. Previous research demonstrated the occurrence of the catalytic transformation of nitrosamine precursors to yield nitrosamines on the surface of activated carbon under environmentally relevant conditions (Padhye et al. 2010; Padhye et al. 2011). Adsorption of chlorpheniramine and catalytic reactions such as degradation forming nitrosamine FPs could simultaneously occur on the surface of GO-Fe_3O_4.

Removal of nitrosamine FPs posed by chlorpheniramine in deionized water

Padhye et al. reported that on the surface of activated carbon, dissolved oxygen forms reactive oxygen species (ROS), further reacting with dissolved nitrogen to form reactive nitrogen species (RNS) such as N_2O, H_2N_2O, and NH_2OH and catalyzing NDMA formation from secondary amines (Padhye et al. 2010; Padhye et al. 2011). The formation of ROS on the surface of GO was reported (Chang et al. 2011; Zhao et al. 2014). In this study, the experiments were conducted to investigate whether chlorpheniramine adsorption and degradation reaction simultaneously occurred increasing the NDMA and/or other nitrosamine FPs in wastewater.

Table 3 lists the NDMA-FP variations in deionized water with the addition of chlorpheniramine before and after the adsorption by GO-Fe_3O_4. In the results, the molar yields of NDMA-FPs

Table 3 NDMA-FP variations in deionized water spiked with chlorpheniramine before and after the adsorption by the GO-Fe₃O₄

Chlorpheniramine (μM)	Before adsorption		After adsorption	
	NDMA-FP (ng/L)	Molar yield (%)	NDMA-FP (ng/L)	NDMA-FP increase (ng/mg GO)
7.3	5441.3 ± 63.7	1.01%	7480.9 ± 549.5	37.1
14.6	13,559.0 ± 361.1	1.25%	14,448 ± 1219.4	85.0

(1.01–1.25%) by adding chlorpheniramine were similar to those reported in publications (Liu et al. 2014; Shen and Andrews 2011a; Shen and Andrews 2011b). However, after the adsorption by GO-Fe₃O₄, the NDMA-FP in the water was not removed and was elevated by 6.6–37.5%. The increase of NDMA-FP of chlorpheniramine by adding GO-Fe₃O₄ ranged from 37.1 to 85.0 ng/mg. The results suggested that chlorpheniramine was potentially removed by adsorption and/or degradation reaction, as the later process could form NDMA precursors increasing the NDMA- and/or nitrosamine FPs (e.g., those observed in Fig. 4).

Conclusion

Chlorpheniramine is a pharmaceutical pollutant and a precursor of carcinogenic nitrosamines. Given the efficient adsorption of chlorpheniramine onto GO-Fe₃O₄ in deionized water, the maximum adsorption of chlorpheniramine in wastewaters decreased in the order: GO-Fe₃O₄ suspension > GO-Fe₃O₄ particles > activated carbon. Chlorpheniramine adsorption on GO-Fe₃O₄ particles and activated carbon was reduced by using real wastewaters as the background, whereas the chlorpheniramine adsorption on GO-Fe₃O₄ suspension was enhanced due to the effects of surface charge on GO-Fe₃O₄ and ionic strength variation in waters. Appreciable levels of NDMA and other nitrosamine FP removals were observed when GO-Fe₃O₄ was used in real wastewaters. However, when chlorpheniramine was present in wastewaters, the chlorpheniramine adsorption and degradation reaction potentially occurred on the surface of GO-Fe₃O₄, increasing NDMA and other nitrosamine FPs in wastewaters after the addition of GO-Fe₃O₄ for chlorpheniramine removal. Similar results were observed by analyzing the variation of NDMA-FP during chlorpheniramine adsorption on the GO-Fe₃O₄ in deionized water. GO-Fe₃O₄ is a potential adsorbent for chlorpheniramine removal. Nevertheless, the low treatment efficiencies at high doses limit its application for nitrosamine FP adsorptions in real wastewaters.

Compliance with ethical standards

Disclaimer Its contents are solely the responsibility of the authors and do not necessarily represent the official views of the MOST.

References

Apul OG, Wang QL, Zhou Y, Karanfil T (2013) Adsorption of aromatic organic contaminants by graphene nanosheets: comparison with carbon nanotubes and activated carbon. Water Res 47:1648–1654

Bond T, Templeton MR, Graham N (2012) Precursors of nitrogenous disinfection by-products in drinking water-a critical review and analysis. J Hazard Mater 235:1–16

Boxall ABA (2004) The environmental side effects of medication - how are human and veterinary medicines in soils and water bodies affecting human and environmental health? EMBO Rep 5:1110–1116

Carter MC, Kilduff JE, Weber WJ (1995) Site energy-distribution analysis of preloaded adsorbents. Environ Sci Technol 29:1773–1780

Chang YL, Yang ST, Liu JH, Dong E, Wang YW, Cao AN, Liu YF, Wang HF (2011) In vitro toxicity evaluation of graphene oxide on A549 cells. Toxicol Lett 200:201–210

Chen S, Zhu J, Wu X, Han Q, Wang X (2010) Graphene Oxide-MnO2 Nanocomposites for Supercapacitors. ACS Nano 4:2822–2830

Chen C, Leavey S, Krasner SW, Suffet IH (2014) Applying polarity rapid assessment method and ultrafiltration to characterize NDMA precursors in wastewater effluents. Water Res 57:115–126

Chen WH, Yang YC, Wang YH, Li CM, Lin KY, Lou JC (2015) Effect of molecular characteristics on the formation of nitrosamines during chlor(am)ination of phenylurea herbicides. Environ Sci Processes Impacts 17:2092–2100

Chen WH, Wang CY, Huang TH (2016) Formation and fates of nitrosamines and their formation potentials from a surface water source to drinking water treatment plants in southern Taiwan. Chemosphere 161:546–554

Chen WH, Huang TH, Wang CY (2018) Impact of pre-oxidation on nitrosamine formation from a source to drinking water: a perspective on cancer risk assessment. Process Saf Environ Prot 113:424–434

Chung K, Lee C-H, Yi G-C (2010) Transferable GaN layers grown on ZnO-coated graphene layers for optoelectronic devices. Science 330:655–657

Fan Z, Yan J, Wei T, Zhi L, Ning G, Li T, Wei F (2011) Asymmetric supercapacitors based on graphene/MnO2 and activated carbon nanofiber electrodes with high power and energy density. Adv Funct Mater 21:2366–2375

Fan LL, Luo CN, Sun M, Qiu HM, Li XJ (2013) Synthesis of magnetic beta-cyclodextrin-chitosan/graphene oxide as nanoadsorbent and its application in dye adsorption and removal. Colloids Surf B Biointerfaces 103:601–607

Geim AK, Novoselov KS (2007) The rise of graphene. Nat Mater 6:183–191

Hanigan D, Zhang J, Herckes P, Krasner SW, Chen C, Westerhoff P (2012) Adsorption of N-Nitrosodimethylamine precursors by

powdered and granular activated carbon. Environ Sci Technol 46: 12630–12639

IARC (1987) IARC monographs on the evaluation of carcinogenic risks to humans, overall evaluations of carcinogenicity: an updating of IARC monographs volumes 1 to 42. International Agency for Research on Cancer, World Health Organization (WHO), Lyon, France

Kadmi Y, Favier L, Wolbert D (2015) N-nitrosamines, emerging disinfection by-products of health concern: an overview of occurrence, mechanisms of formation, control and analysis in water. Water Sci Technol Water Supply 15:11–25

Krasner SW, Mitch WA, McCurry DL, Hanigan D, Westerhoff P (2013) Formation, precursors, control, and occurrence of nitrosamines in drinking water: a review. Water Res 47:4433–4450

Lee J, Chae HR, Won YJ, Lee K, Lee CH, Lee HH, Kim IC, Lee JM (2013) Graphene oxide nanoplatelets composite membrane with hydrophilic and antifouling properties for wastewater treatment. J Membr Sci 448:223–230

Li Z, Chang P-H, Jean J-S, Jiang W-T, Hong H (2011) Mechanism of chlorpheniramine adsorption on Ca-montmorillonite. Colloids Surf a-Physicochemical Eng Asp 385:213–218

Li J, Zhang S, Chen C, Zhao G, Yang X, Li J, Wang X (2012) Removal of Cu(II) and fulvic acid by graphene oxide nanosheets decorated with Fe3O4 nanoparticles. ACS Appl Mater Interfaces 4:4991–5000

Li CM, Chen CH, Chen WH (2017) Different influences of nanopore dimension and pH between chlorpheniramine adsorptions on graphene oxide-iron oxide suspension and particle. Chem Eng J 307:447–455

Lin YX, Xu S, Jia L (2013) Fast and highly efficient tetracyclines removal from environmental waters by graphene oxide functionalized magnetic particles. Chem Eng J 225:679–685

Liu YD, Selbes M, Zeng CC, Zhong RG, Karanfil T (2014) Formation mechanism of NDMA from ranitidine, trimethylamine, and other tertiary amines during chloramination: a computational study. Environ Sci Technol 48:8653–8663

Luo YB, Shi ZG, Gao QA, Feng YQ (2011) Magnetic retrieval of graphene: extraction of sulfonamide antibiotics from environmental water samples. J Chromatogr A 1218:1353–1358

Lv J, Wang L, Song Y, Li Y (2015) N-nitrosodimethylamine formation from ozonation of chlorpheniramine: influencing factors and transformation mechanism. J Hazard Mater 299:584–594

Mitch WA, Oelker GL, Hawley EL, Deeb RA, Sedlak DL (2005) Minimization of NDMA formation during chlorine disinfection of municipal wastewater by application of pre-formed chloramines. Environ Eng Sci 22:882–890

Moreno RA, Oliveira-Silva D, Sverdloff CE, Borges BC, Galvinas PAR, Astigarraga RB, Borges NC (2010) Determination of chlorpheniramine in human plasma by HPLC-ESI-MS/MS: application to a dexchlorpheniramine comparative bioavailability study. Biomed Chromatogr 24:774–781

Padhye L, Wang P, Karanfil T, Huang C-H (2010) Unexpected role of activated carbon in promoting transformation of secondary amines to N-nitrosamines. Environ Sci Technol 44:4161–4168

Padhye LP, Hertzberg B, Yushin G, Huang C-H (2011) N-nitrosamines formation from secondary amines by nitrogen fixation on the surface of activated carbon. Environ Sci Technol 45:8368–8376

Roberts J, Kumar A, Du J, Hepplewhite C, Ellis DJ, Christy AG, Beavis SG (2016) Pharmaceuticals and personal care products (PPCPs) in Australia's largest inland sewage treatment plant, and its contribution to a major Australian river during high and low flow. Sci Total Environ 541:1625–1637

Sacher F, Schmidt C, Lee C, von Gunten U (2008) Strategies for minimizing nitrosamine formation during disinfection. Awwa Research Foundation, Alexandria

Schlautman MA, Morgan JJ (1993) Effects of aqueous chemistry on the binding of polycyclic aromatic-hydrocarbons by dissolved humic materials. Environ Sci Technol 27:961–969

Schwarzenbach RP, Gschwend PM, Imboden DM (2003) Environmental organic chemistry. John Wiley & Sons, Inc., New Jersey, U.S.A.

Shah AD, Krasner SW, Lee CFT, von Gunten U, Mitch WA (2012) Trade-offs in disinfection byproduct formation associated with precursor preoxidation for control of N-nitrosodimethylamine formation. Environ Sci Technol 46:4809–4818

Shen R, Andrews SA (2011a) Demonstration of 20 pharmaceuticals and personal care products (PPCPs) as nitrosamine precursors during chloramine disinfection. Water Res 45:944–952

Shen RQ, Andrews SA (2011b) NDMA formation kinetics from three pharmaceuticals in four water matrices. Water Res 45:5687–5694

Stankovich S, Dikin DA, Dommett GHB, Kohlhaas KM, Zimney EJ, Stach EA, Piner RD, Nguyen ST, Ruoff RS (2006) Graphene-based composite materials. Nature 442:282–286

Takeuchi H, Yamashita N, Nakada N, Tanaka H (2018) Removal characteristics of N-nitrosamines and their precursors by pilot-scale integrated membrane Systems for Water Reuse. Int J Environ Res Public Health 15. https://doi.org/10.3390/ijerph15091960

USEPA (2004) Method 521: determination of nitrosamines in drinking water by solid phase extraction and capillary column gas chromatography with large volume injection and chemical ionization tandem mass spectrometry (MS/MS). USEPA, Cincinnati, Ohio

USEPA (2017): Integrated risk information system (IRIS). U.S. Environmental Protection Agency (USEPA)

Uzun H, Kim D, Karanfil T (2017) The removal of N-nitrosodimethylamine formation potential in drinking water treatment plants. J Am Water Works Assoc 109:15–28

Wang WF, Yu JW, An W, Yang M (2016) Occurrence and profiling of multiple nitrosamines in source water and drinking water of China. Sci Total Environ 551:489–495

Wu Y, Li Z, Chen J, Yu C, Huang X, Zhao C, Duan L, Yang Y, Lu W (2015) Graphene nanosheets decorated with tunable magnetic nanoparticles and their efficiency of wastewater treatment. Mater Res Bull 68:234–239

Xia C, Lv GC, Mei LF, Song KN, Li ZH, Wang XY, Xing XB, Xu B (2014) Removal of Chlorpheniramine from water by Birnessite. Water Air Soil Pollut 225

Yang L, Chen ZL, Shen JM, Xu ZZ, Liang H, Tian JY, Ben Y, Zhai X, Shi WX, Li GB (2009) Reinvestigation of the nitrosamine-formation mechanism during ozonation. Environ Sci Technol 43:5481–5487

Yang Z, Yan H, Yang H, Li HB, Li AM, Cheng RS (2013) Flocculation performance and mechanism of graphene oxide for removal of various contaminants from water. Water Res 47:3037–3046

Zhang Y, Li H, Pan L, Lu T, Sun Z (2009) Capacitive behavior of graphene-ZnO composite film for supercapacitors. J Electroanal Chem 634:68–71

Zhao J, Wang Z, White JC, Xing B (2014) Graphene in the aquatic environment: adsorption, dispersion, toxicity and transformation. Environ Sci Technol 48:9995–10009

Zhou WJ, Chen CP, Lou LJ, Yang Q, Zhu LZ (2014) Formation potential of nine nitrosamines from corresponding secondary amines by chloramination. Chemosphere 95:81–87